Proton Conducting Materials

DOI: 10.1002/anie.201404164

pH-Dependent Proton Conducting Behavior in a Metal–Organic Framework Material**

*Won Ju Phang, Woo Ram Lee, Kicheon Yoo, Dae Won Ryu, BongSoo Kim, and Chang Seop Hong**

Abstract: *A porous metal–organic framework (MOF), [Ni_2(dobdc)(H_2O)$_2$]·6H_2O (Ni_2(dobdc) or Ni-MOF-74; dobdc^{4-} = 2,5-dioxido-1,4-benzenedicarboxylate) with hexagonal channels was synthesized using a microwave-assisted solvothermal reaction. Soaking Ni_2(dobdc) in sulfuric acid solutions at different pH values afforded new proton-conducting frameworks, H^+@Ni_2(dobdc). At pH 1.8, the acidified MOF shows proton conductivity of 2.2×10^{-2} S cm^{-1} at 80 °C and 95 % relative humidity (RH), approaching the highest values reported for MOFs. Proton conduction occurs via the Grotthuss mechanism with a significantly low activation energy as compared to other proton-conducting MOFs. Protonated water clusters within the pores of H^+@Ni_2(dobdc) play an important role in the conduction process.*

Among various fuel cells, the most promising candidate for transportation applications is the proton exchange membrane fuel cell (PEMFC).[1] In a fuel cell, the oxidized protons produced at the anode travel through the membrane electrolyte and combine with oxygen at the cathode in the presence of electrons from the external circuit. This process emits minimal environmental pollutants because the electrochemical reaction produces only water as the byproduct. The membrane materials should be specifically designed to allow the exclusive diffusion of protons. Nafion, a perfluoro-sulfonated copolymer, has been shown to be the best-performing membrane electrolyte in PEMFCs with high proton conductivity.[1] This polymer requires humid environments to transport protons, and thereby operates efficiently below 80 °C.

Metal–organic frameworks (MOFs) with a high surface area have potential applications in gas storage and separation, catalysis, and other fields.[2] Their advantages include modular synthesis and a tunable porosity, which can be controlled by the facile modifications of organic linkers and special groups grafted onto open metal sites. Due to the tunability of pore sizes, shapes, and functionalities, MOFs have emerged as a new type of ion conductor. A growing number of proton-conducting MOFs have been recently reported,[3] and the research targets are generally classified into two categories: water-mediated proton-conducting MOFs operating below 100 °C and anhydrous proton conductors operating above 100 °C. Recent advances in conductive MOFs have been focused on elucidating the underlying proton transport mechanism under different chemical circumstances[4] as well as on developing innovative materials with conductivities approaching those of conventional materials such as sulfonated polymers, polybenzimidazole-based electrolytes, solid acids, and ceramic oxides.[1,3b]

To allow protons to readily move through a framework, proton donors and acceptors must be closely positioned to build conduction pathways, and the protonation and deprotonation events between the pertinent sites must also occur favorably. The introduction of acidic groups into a material improves the proton conduction because they serve as proton sources that confer protons to hydrogen-bonded proton conducting routes. Thus, the membrane electrolytes of choice should contain acidic moieties (e.g. sulfonic acid, phosphoric acid, carboxylic acid, ammonium) linked to the framework backbones[4a,5] or guest molecules (e.g. imidazole, triazole, histamine)[6] embedded in the pores. The mesoporous material MIL-101 impregnated with nonvolatile sulfuric acid (H_2SO_4) and phosphoric acid (H_3PO_4) was recently reported to have high proton conductivities at 150 °C and low humidity.[7] The conducting properties of hybrid materials depend on the K_a values of the acids, and conductivities of the substituted MIL-53 derivatives were found to vary in the order of pK_a values of *meta*-substituted benzoic acids.[4a]

Since proton conductivity is determined partly by the amount of protonic charge carriers, it is imperative to develop methods to increase the proton concentration in a material. A strong acid can be fully ionized in an aqueous solution and H^+ can be directly supplied to the MOF of interest. In this situation, self-dissociation of the acid to H^+ is not required during proton conduction, thereby enabling a significant rise in conductivity. Therefore, although this has not been previously documented, it is envisioned that pH can be adjusted to increase the proton concentration and consequently optimize conduction properties of a material.[5i,8] The essential requirement for this method to work is that the framework of the material should survive under the acidic conditions used.

Here, we employed nanoporous MOF Ni_2(dobdc) possessing 1D hexagonal channels with a diameter of 11 Å, which remains intact at pH values as low as 1.8. Ni_2(dobdc) shows a proton conductivity of 1.4×10^{-4} S cm^{-1} at 80 °C and 95 %

[*] W. J. Phang, W. R. Lee, D. W. Ryu, Prof. C. S. Hong
Department of Chemistry, Korea University
Seoul 136-713 (Korea)
E-mail: cshong@korea.ac.kr
K. Yoo, Dr. B. Kim
Photo-electronic Hybrids Research Center
Korea Institute of Science and Technology (KIST)
Seoul 136-791 (Korea)

[**] This work was supported by a Korea CCS R&D Center (KCRC) grant funded by the Korean government (The Ministry of Science, ICT & Future Planning (MSIP)) (NRF-2013M1A8A1035849).

Supporting information for this article is available on the WWW under http://dx.doi.org/10.1002/anie.201404164.

relative humidity (RH). Treatment of Ni_2(dobdc) with sulfuric acid solutions of various concentrations drastically increases proton conduction. At pH 1.8, the conductivity of the acidified framework H^+@Ni_2(dobdc) reaches 2.2×10^{-2} S cm^{-1} at 80 °C and 95 % RH, which is two orders of magnitude larger than that of as-prepared Ni_2(dobdc) and is among the highest values reported for MOFs. Remarkably, the activation energy of this system marks one of the lowest values for conductive MOFs. For the first time, we demonstrate pH-dependent proton conductivity in proton-conducting MOFs.

A microwave-assisted reaction of Ni^{2+} and H_4dobdc in THF/H_2O was employed at 110 °C with 80 psi and 100 W, producing yellow powders of Ni_2(dobdc). The microwave synthesis of Ni_2(dobdc) significantly reduced the reaction time (15 min) when compared with conventional solvothermal synthesis (3 days),[9] due to rapid nucleation and crystal growth accelerated by microwave irradiation. The phase formation of as-prepared Ni_2(dobdc) was verified by the PXRD profile that matches well with the simulated curve (Figure 1c). A potential proton-conducting material should be stable under humid environments because water is omnipresent in the operation of PEMFCs. We tested the water stability of the as-prepared sample by refluxing it in water at 100 °C for 7 days (Supporting Information, Figure S1). The framework is found to be highly robust even in boiling water.

To examine the chemical stability of Ni_2(dobdc), it was soaked in aqueous solutions of sulfuric acid (H_2SO_4) with various pH values for 3 days at room temperature. The PXRD data show that the framework remains intact until pH 1.8 (Figure 1c and S2). However, additional peaks begin to appear in the PXRD profile at pH 1.8. The framework fully collapses at pH 0.8 to generate a different phase. We tested the pH values of the solutions before and after immersion of the samples and found that the estimated H^+ concentrations of the acidic solids were similar to those of the nominal pH values (Table S1 and Figure S3). The acidified solid H^+@Ni_2-(dobdc) was dispersed in water, and the pH of the supernatant was measured to be almost neutral. This implies that the protons infused into the framework are held tightly within the pores. The SO_4^{2-} species might be present in the acidic framework as counter anions to maintain charge balance. However, the EDX and elemental analysis data indicate that there are no traces of elemental sulfur, confirming the absence of the anion in the sample (Figure S4, Tables S2 and S3). The UV/Vis spectra (Figure S5) indicated that traces of Ni^{2+} leached from the framework, which is responsible for the charge balance of the acidified solid. Therefore, it is probable that the protons, which could be associated with the released anionic dobdc linkers after metal leaching, are present in the channels where water molecules form hydrogen-bonded clusters with them. Thermogravimetric (TG) analysis on the as-prepared and acidified samples reveals that the first decomposition occurs in the temperature range 30–200 °C, which corresponds to coordinated (2 H_2O) and lattice water molecules (6 H_2O). The second decomposition, which starts above 400 °C, is related to the loss of the linked ligands (Figure S6). The decomposition profiles for all the samples

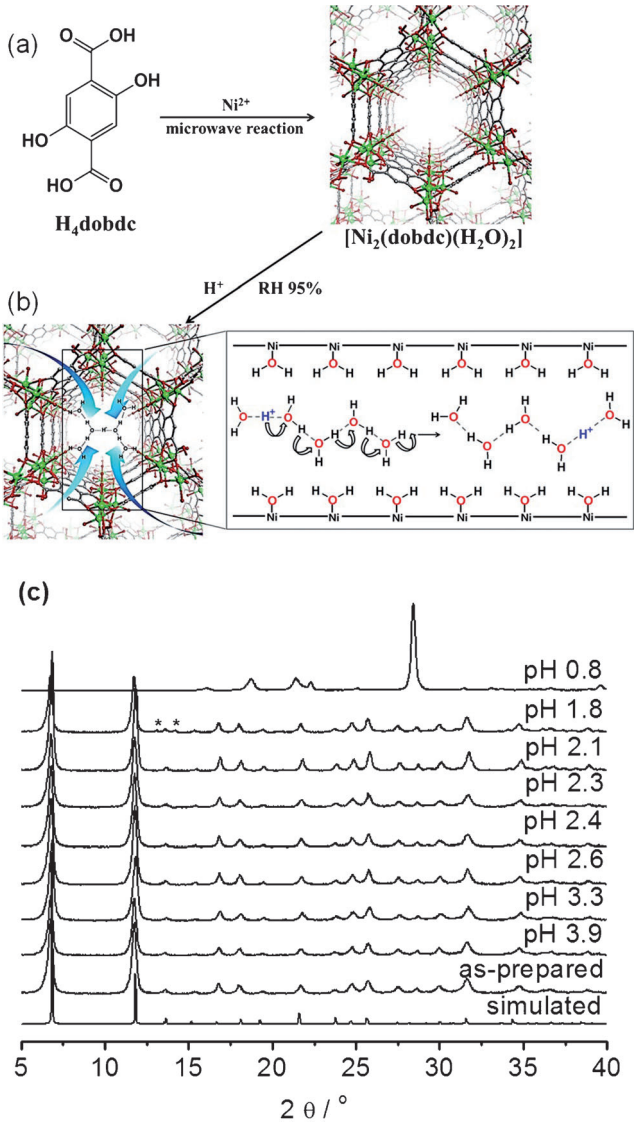

Figure 1. a) Synthesis and structure of Ni_2(dobdc) showing a 1D channel along the *c*-axis. b) Cross-sectional view of the pore with protonated water clusters, illustrating a proposed Grotthuss mechanism inside the channel. c) PXRD data for the simulated, as-prepared, and acidified samples at indicated pH values.

are almost overlapped to each other, suggesting similar thermal stability. Scanning electron microscopy (SEM) images display that the as-prepared and pH 2.4 samples have analogous grain sizes (Figure S7).

To inspect the proton conductivity (σ), AC impedance analysis was carried out using pellets of multiple samples at several pH conditions (Figure 2, S8–S13, and Table S4). The conductivity contributed from bulk and grain boundary is not resolved because only one minimum is observed in each plot. The σ value of the as-prepared Ni_2(dobdc) at 25 °C and 95 % RH is found to be 5.3×10^{-5} S cm^{-1} from the Nyquist plot. With increasing temperature, σ continues to rise and reach 1.4×10^{-4} S cm^{-1} at 80 °C. The conductive protons are initially supplied by the polarized water molecules bound to open metal sites, and they travel through the pores with the

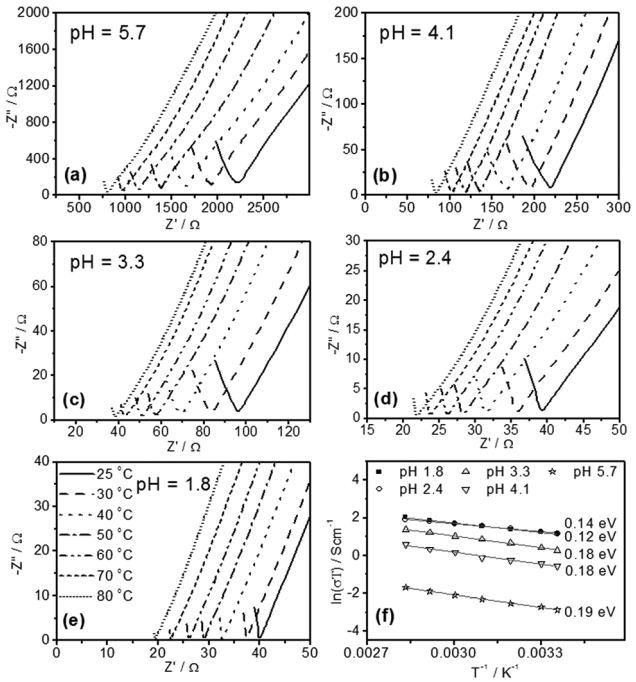

Figure 2. Nyquist plots of H^+@Ni_2(dobdc) at a) pH 5.7, b) pH 4.1, c) pH 3.3, d) pH 2.4, and e) pH 1.8 at various temperatures and 95% RH condition. f) Arrhenius plots of proton conductivities.

assistance of hydrogen-bonded lattice water molecules.[4b] The σ value exceeds that (10^{-9}) observed for Zn-MOF-74 accommodating histamine molecules in the pores under anhydrous conditions.[6d] The poor conduction behavior in the Zn-MOF-74 framework was attributed to the poor proton hopping between imidazole groups. The enhanced σ in Ni_2-(dobdc) suggests that the water-mediated conduction occurs more easily along the channels of the MOF-74 type structure.

We also measured the conduction properties of H^+@Ni_2-(dobdc) under humidified conditions. The conductivity drastically increases with pH: At 25 °C, σ is 1.9×10^{-4} S cm^{-1} at pH 5.7, 1.9×10^{-3} S cm^{-1} at pH 4.1, 4.5×10^{-3} S cm^{-1} at pH 3.3, and 1.1×10^{-2} S cm^{-1} at pH 2.4, and 1.1×10^{-2} S cm^{-1} at pH 1.8. The value at 80 °C is found to be even greater, being 5.3×10^{-4} S cm^{-1} at pH 5.7, 5.1×10^{-3} S cm^{-1} at pH 4.1, 1.3×10^{-2} S cm^{-1} at pH 3.3, 1.9×10^{-2} S cm^{-1} at pH 2.4, and 2.2×10^{-2} S cm^{-1} at pH 1.8. Notably, the conductivity (2.2×10^{-2} S cm^{-1}) of the acidified sample at pH 1.8 is exceptionally high and among the highest values reported for MOFs such as $[(Me_2NH_2)_3(SO_4)]_2[Zn_2(ox)_3]$ with 4.2×10^{-2} S cm^{-1} at 25 °C and 98% RH,[10] PCMOF2^1/$_2$ showing $\sigma = 2.1\times10^{-2}$ S cm^{-1} at 85 °C and 90% RH,[5c] and H_2SO_4@MIL-101 with 1×10^{-2} S cm^{-1} at 150 °C and 0.13% RH (Table S5).[7]

Besides high conductivity, it is important to devise a system with lower activation energy (E_a). Materials with low E_a remains almost invariant to temperature, a property required for fuel cell applications. E_a of proton transport was extracted by utilizing the linear correlation in the plot of $\ln(\sigma T)$ versus $1/T$. E_a is estimated to be in the range 0.12–0.20 eV, which is relatively low compared to Nafion (0.22 eV),[11] uranium phosphate (0.32 eV),[12] and most of the previously reported proton-conducting MOFs (Table S5). The recognized gap in E_a is detectable between samples at pH 2.4 and the others, which may be relevant to the critical mass change of proton at the point. Particularly, E_a (0.12 eV) at pH 2.4 is among the lowest values observed for the relevant conducting MOFs (Table S5), as exemplified by In-5TIA (0.14 eV)[13] and PCMOF-5 (0.16 eV).[5i] From the result, highly efficient proton transfer takes place via the Grotthuss mechanism, in which the protons pass through the pores of the acidified material. The proton-transport Grotthuss mechanism is suggested to involve two modes of protonated water clusters, hydrated hydronium called Eigen cation H_3O^+-$(H_2O)_3$ and the intermediate proton dihydrate called Zundel ion $H_2O\cdots H^+\cdots OH_2$ between Eigen cations.[14] In the acidified samples, it is not necessary to dissociate H^+ for proton donation, contrary to the case of most ion-conducting MOFs that necessitate such a dissociation process.[4a] Fully liberated protons were included in the framework without SO_4^{2-} anions, as already proved by EDX. The free protons bind to associated water molecules, giving rise to protonated water clusters $H^+(H_2O)_n$ of diverse sizes and types (Eigen and Zundel ions) resulting in superior conduction. Thus, the 1D channels in this system provide well organized conduction pathways for a proton to hop from one site to another, and is responsible for the apparent low energy barrier.

To probe the effect of humidity on proton conduction, we measured σ as a function of RH and temperature (Figure S14 and S15). The σ value for the as-prepared and pH 2.4 samples decreases with decreasing RH. For the pH 2.4 sample at 60% RH, E_a is estimated at 0.20 eV. Some loss of water molecules under low humid conditions may account for this observation because the defect sites compel each proton to travel over a longer distance. Lower values of humidity are thus accompanied by a higher energy barrier, as evidenced by the increase in E_a from 0.12 eV at 95% RH to 0.20 eV at 60% RH. The PXRD data point out that the materials retain their structural integrity even after the conductivity measurements (Figure S16). Before and after the conductivity measurements, the samples were heated at 300 °C in vacuum to remove most water molecules, and the gases were adsorbed on the activated samples (Figure S17). Similar gas uptakes reveal that the pore structures are well maintained. The water adsorption curves for the as-prepared and pH 2.1 samples were obtained after treating them at 250 °C for 2 h (Figure S18). The acidified material turns out to be more hydrophilic than the as-prepared one because more water molecules are adsorbed at a faster rate for the pH 2.1 sample. This hydrophilicity is associated with the enhanced proton conduction in the materials of lower pH (Figure 3).[5d,f]

In order to examine the protonated water environment of the material, IR spectra were recorded at different pH. The samples were heated at 100 °C for 2 h to eliminate the surface attached water molecules before the measurements. They were put in an air-tight IR cell (NaCl windows) in a dry box filled with Ar. The cell was isolated from the air with an oil bubbler to prevent the influx of ambient humidity. For the as-prepared sample, the characteristic O–H stretching vibrations of water molecules are evident at 3660 and 3572 cm^{-1}. Compared to these absorption bands, the O–H peaks in the acidified samples are red-shifted to lower wavenumbers with

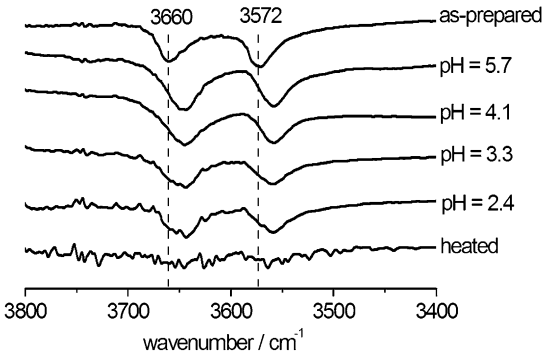

Figure 3. IR spectra of as-prepared Ni_2(dobdc), H^+@Ni_2(dobdc) at different pH values, and H^+@Ni_2(dobdc) after heating the sample at 300 °C.

bands at 3644 and 3558 cm^{-1}. In the hydrogen bonded system $H_2O\cdots HOH$, the neighboring O–H covalent bonds are prone to be weaker as the O···H interaction becomes stronger.[15] For a protonated water cluster $H^+(H_2O)_n$, the hydrogen bonding interaction in the inner shell closer to H^+ is progressively stronger than that in the bulk, resulting in weakening of the O–H stretch frequency, as observed in the IR absorption bands for the acidified samples.[16] In the given pH range, the position of the O–H peaks is nearly identical. Protonated water clusters with $n > 6$ calculated using the clusters-in-liquid method was suggested to exhibit the O–H stretch bands at the similar frequencies.[17] Considering that the acidified samples have $n \gg 6$, the observation is consistent with the cluster model. The peaks in the O–H stretch region fade away when all the water molecules were removed under vacuum at 300 °C for 2 h, indicating the origin of absorption bands above 3400 cm^{-1}. Hence, it is clear that the protonated water clusters play a crucial role in proton transport along the pores. Since the conductivity is partly proportional to the concentration of H^+ ions, lower pH values donate more protons to the system, thus promoting proton conductivity, as observed in the present case. In addition, from the RH dependence plots (Figure S14b), the as-prepared sample with low H^+ concentration engenders rapid increase above 85% RH, while a sample including high proton density (pH 2.4, for instance) shows steep rise at 75% RH. These data would be a good hint for the correlation between proton density and proton conductivity, and evidence of Grotthuss type proton transportation mechanism (Figure 1b and S19).

In summary, the porous framework Ni_2(dobdc) with hexagonal channels was prepared using microwave-assisted synthesis. The material is found to be robust in boiling water for 7 days and in acidic solutions with pH as low as pH 1.8. We have demonstrated for the first time, the direct introduction of H^+ into the material to create proton-conducting MOFs. The acidified MOF H^+@Ni_2(dobdc) at pH 1.8 exhibits a significant proton conductivity of 2.2×10^{-2} S cm^{-1}, which is comparable to the highest values reported for MOFs. The proton transfer occurs via the Grotthuss mechanism with the lowest energy barrier for proton hopping, which involves protonated water clusters present within the channels. Further studies to probe the location of protons in the framework could be required for understanding of the possible mechanism of proton conduction in this system. The foregoing results constitute a promising new strategy for perusing high-performance proton conducting materials.

Received: April 10, 2014
Revised: May 13, 2014
Published online: July 1, 2014

Keywords: metal–organic frameworks · proton conducting materials · protonated water clusters

[1] C. Laberty-Robert, K. Valle, F. Pereira, C. Sanchez, *Chem. Soc. Rev.* **2011**, *40*, 961 – 1005.
[2] a) Y. Cui, Y. Yue, G. Qian, B. Chen, *Chem. Rev.* **2012**, *112*, 1126 – 1162; b) L. E. Kreno, K. Leong, O. K. Farha, M. Allendorf, R. P. Van Duyne, J. T. Hupp, *Chem. Rev.* **2012**, *112*, 1105 – 1125; c) J. R. Li, J. Sculley, H. C. Zhou, *Chem. Rev.* **2012**, *112*, 869 – 932; d) K. Sumida, D. L. Rogow, J. A. Mason, T. M. McDonald, E. D. Bloch, Z. R. Herm, T. H. Bae, J. R. Long, *Chem. Rev.* **2012**, *112*, 724 – 781; e) M. Yoon, R. Srirambalaji, K. Kim, *Chem. Rev.* **2012**, *112*, 1196 – 1231.
[3] a) S. Li, Q. Xu, *Energy Environ. Sci.* **2013**, *6*, 1656 – 1683; b) M. Yoon, K. Suh, S. Natarajan, K. Kim, *Angew. Chem.* **2013**, *125*, 2752 – 2764; *Angew. Chem. Int. Ed.* **2013**, *52*, 2688 – 2700.
[4] a) A. Shigematsu, T. Yamada, H. Kitagawa, *J. Am. Chem. Soc.* **2011**, *133*, 2034 – 2036; b) N. C. Jeong, B. Samanta, C. Y. Lee, O. K. Farha, J. T. Hupp, *J. Am. Chem. Soc.* **2012**, *134*, 51 – 54.
[5] a) R. M. Colodrero, P. Olivera-Pastor, E. R. Losilla, D. Hernandez-Alonso, M. A. Aranda, L. Leon-Reina, J. Rius, K. D. Demadis, B. Moreau, D. Villemin, M. Palomino, F. Rey, A. Cabeza, *Inorg. Chem.* **2012**, *51*, 7689 – 7698; b) R. M. P. Colodrero, K. E. Papathanasiou, N. Stavgianoudaki, P. Olivera-Pastor, E. R. Losilla, M. A. G. Aranda, L. León-Reina, J. Sanz, I. Sobrados, D. Choquesillo-Lazarte, J. M. García-Ruiz, P. Atienzar, F. Rey, K. D. Demadis, A. Cabeza, *Chem. Mater.* **2012**, *24*, 3780 – 3792; c) S. Kim, K. W. Dawson, B. S. Gelfand, J. M. Taylor, G. K. Shimizu, *J. Am. Chem. Soc.* **2013**, *135*, 963 – 966; d) H. Okawa, M. Sadakiyo, T. Yamada, M. Maesato, M. Ohba, H. Kitagawa, *J. Am. Chem. Soc.* **2013**, *135*, 2256 – 2262; e) E. Pardo, C. Train, G. Gontard, K. Boubekeur, O. Fabelo, H. Liu, B. Dkhil, F. Lloret, K. Nakagawa, H. Tokoro, S. Ohkoshi, M. Verdaguer, *J. Am. Chem. Soc.* **2011**, *133*, 15328 – 15331; f) M. Sadakiyo, H. Ōkawa, A. Shigematsu, M. Ohba, T. Yamada, H. Kitagawa, *J. Am. Chem. Soc.* **2012**, *134*, 5472 – 5475; g) M. Sadakiyo, T. Yamada, H. Kitagawa, *J. Am. Chem. Soc.* **2009**, *131*, 9906 – 9907; h) S. Sen, N. N. Nair, T. Yamada, H. Kitagawa, P. K. Bharadwaj, *J. Am. Chem. Soc.* **2012**, *134*, 19432 – 19437; i) J. M. Taylor, K. W. Dawson, G. K. Shimizu, *J. Am. Chem. Soc.* **2013**, *135*, 1193 – 1196; j) J. M. Taylor, R. K. Mah, I. L. Moudrakovski, C. I. Ratcliffe, R. Vaidhyanathan, G. K. H. Shimizu, *J. Am. Chem. Soc.* **2010**, *132*, 14055 – 14057; k) D. Umeyama, S. Horike, M. Inukai, T. Itakura, S. Kitagawa, *J. Am. Chem. Soc.* **2012**, *134*, 12780 – 12785; l) T. Yamada, M. Sadakiyo, H. Kitagawa, *J. Am. Chem. Soc.* **2009**, *131*, 3144 – 3145; m) T. Kundu, S. C. Sahoo, R. Banerjee, *Chem. Commun.* **2012**, *48*, 4998 – 5000; n) T. Panda, T. Kundu, R. Banerjee, *Chem. Commun.* **2013**, *49*, 6197 – 6199.
[6] a) D. Umeyama, S. Horike, M. Inukai, Y. Hijikata, S. Kitagawa, *Angew. Chem.* **2011**, *123*, 11910 – 11913; *Angew. Chem. Int. Ed.* **2011**, *50*, 11706 – 11709; b) J. A. Hurd, R. Vaidhyanathan, V. Thangadurai, C. I. Ratcliffe, I. L. Moudrakovski, G. K. H. Shimizu, *Nat. Chem.* **2009**, *1*, 705 – 710; c) S. Bureekaew, S. Horike, M. Higuchi, M. Mizuno, T. Kawamura, D. Tanaka, N. Yanai, S. Kitagawa, *Nat. Mater.* **2009**, *8*, 831 – 836; d) M. Inukai, S. Horike, D. Umeyama, Y. Hijikata, S. Kitagawa, *Dalton Trans.* **2012**, *41*,

13261 – 13263; e) W. X. Chen, H. R. Xu, G. L. Zhuang, L. S. Long, R. B. Huang, L. S. Zheng, *Chem. Commun.* **2011**, *47*, 11933 – 11935.
[7] V. G. Ponomareva, K. A. Kovalenko, A. P. Chupakhin, D. N. Dybtsev, E. S. Shutova, V. P. Fedin, *J. Am. Chem. Soc.* **2012**, *134*, 15640 – 15643.
[8] G. K. Shimizu, J. M. Taylor, S. Kim, *Science* **2013**, *341*, 354 – 355.
[9] P. D. Dietzel, B. Panella, M. Hirscher, R. Blom, H. Fjellvag, *Chem. Commun.* **2006**, 959 – 961.
[10] S. S. Nagarkar, S. M. Unni, A. Sharma, S. Kurungot, S. K. Ghosh, *Angew. Chem.* **2014**, *126*, 2676 – 2680; *Angew. Chem. Int. Ed.* **2014**, *53*, 2638 – 2642.
[11] a) G. Alberti, M. Casciola, *Solid State Ionics* **2001**, *146*, 3 – 16; b) K. D. Kreuer, S. J. Paddison, E. Spohr, M. Schuster, *Chem. Rev.* **2004**, *104*, 4637 – 4678.
[12] A. T. Howe, M. G. Shilton, *J. Solid State Chem.* **1979**, *28*, 345 – 361.
[13] T. Panda, T. Kundu, R. Banerjee, *Chem. Commun.* **2012**, *48*, 5464 – 5466.
[14] a) N. Agmon, *Chem. Phys. Lett.* **1995**, *244*, 456 – 462; b) O. Markovitch, H. Chen, S. Izvekov, F. Paesani, G. A. Voth, N. Agmon, *J. Phys. Chem. B* **2008**, *112*, 9456 – 9466; c) D. Marx, M. E. Tuckerman, J. Hutter, M. Parrinello, *Nature* **1999**, *397*, 601 – 604.
[15] K. Nakamoto, M. Margoshes, R. E. Rundle, *J. Am. Chem. Soc.* **1955**, *77*, 6480 – 6486.
[16] O. Markovitch, N. Agmon, *J. Phys. Chem. A* **2007**, *111*, 2253 – 2256.
[17] W. Kulig, N. Agmon, *Nat. Chem.* **2013**, *5*, 29 – 35.

